

# Quantitative Evaluation of Renal Cortex Perfusion using Contrast-enhanced Ultrasound Imaging Parameters in Renal Ischemia-reperfusion Injury in Rabbits

zhijian luo

Affiliated Hospital of Southwest Medical University

yulu liu

Southwest Medical University

Ziyi tang

Southwest Medical University

Jialing liu

Southwest Medical University

Xuemei xu

Southwest Medical University

yan dai (✉ [daiyan@swmu.edu.cn](mailto:daiyan@swmu.edu.cn))

Affiliated Hospital of Southwest Medical University <https://orcid.org/0000-0003-4056-6204>

Mingxing Li

Affiliated Hospital of Southwest Medical University

---

## Research

**Keywords:** renal ischemia/reperfusion injury, quantitative analysis of contrast-enhanced

**Posted Date:** October 5th, 2020

**DOI:** <https://doi.org/10.21203/rs.3.rs-49462/v1>

**License:**   This work is licensed under a Creative Commons Attribution 4.0 International License.

[Read Full License](#)

---

# Abstract

**Background:** Contrast-enhanced ultrasound (CEUS) can be used as a noninvasive and quantitative diagnostic method to judge the progression of renal ischemia-reperfusion injury. The aim of this study was to evaluate the blood perfusion of renal cortex during ischemia-reperfusion (I/R) injury by quantitative contrast-enhanced ultrasound (CEUS) parameters.

**Materials:** In this experiment, 24 rabbits were randomly divided into following four groups (N=6): sham-operation group, 24-h post-operation of ischemia-reperfusion injury group (24-h I/R), 3-d post-operation of I/R injury group (3-d I/R) and 5-d post-operation of I/R injury group (5-d I/R). The I/R model was surgically established. CEUS was performed via a GE LOGIQ 9 ultrasound machine, and a time-intensity curve (TIC) in the renal cortex was generated for each group. All quantitative CEUS parameters were derived from TIC and included the following: the curve's peak ascending slope (wash-in slope [WIS]), area under the curve (AUC), time-to-peak (TTP), change in perfusion peak intensity (A), and arrival time (AT). Subsequently, we analyzed the changes in these parameters, as well as the correlation between changes in CEUS parameters and pathological parameters.

**Results:** The values of AT, TTP, and WIS of all I/R groups significantly differed from the sham-operation group ( $P < 0.01$ ). However, there was no difference in A and AUC values among the experimental groups ( $P > 0.05$ ). The AT and TTP values peaked at 3 d after I/R surgery, which correlated with the most significant pathological changes at the same time point.

**Conclusions:** Among the quantitative CEUS parameters, AT, TTP, and WIS were found to be sensitive indicators reflecting blood perfusion in renal microcirculation. Hence, these parameters may be useful for dynamically monitoring the severity of tissue damage at the early stage of I/R injury. Collectively, our findings provide compelling evidence for further clinical application of quantitative CEUS analysis.

## Background

Ischemia/reperfusion injury (I/R) is one of the prime reasons of acute kidney injury (AKI), which is principal consideration by critical illness or surgery [1–4]. Various reactive oxygen species (ROS) were produced during Ischemia/reperfusion injury [5], resulting in tubular atrophy, endothelial injury, and cell death caused by renal tubular repair dysfunction [6–8]. Renal hemodynamics in early stage of IRI can provide important clinical significance for acute renal tubular injury [9, 10].

Serum creatinine and blood urea nitrogen (BUN) have typically been used to diagnose AKI. However, these tests only reveal anomalies when kidney function is significantly compromised [11, 12], Hemodynamic abnormalities in kidney is of great significance of pathogenesis of AKI, and diagnostic tools for evaluating renal hemodynamic are especially lacking [13–15]. Therefore, early diagnosis of hemodynamic changes and timely interventions are critical for improving the prognoses of AKI patients [16].

Contrast-enhanced ultrasonography (CEUS) has developed rapidly in recent years. CEUS evaluates the microcirculation and tissue perfusion and has become an important research topic in diagnostic ultrasound imaging. Many previous studies have demonstrated the importance of damage and reconstruction of renal microcirculation in multiple models of kidney disease [17].

In this study, we build model of renal ischemia/reperfusion injury in a rabbit, performed a series of real-time greyscale CUES, analyzed renal cortical blood flow via TICs and corresponding quantitative parameters, and investigated changes in renal cortical blood flow at the early stage of AKI in rabbits. Collectively, our results may support the value of CEUS-based quantitative analysis in the diagnosis of AKI.

## **1. Materials And Methods**

### **1.1 Animal groups**

Twenty-four healthy adult male rabbits, with average bodyweight differences within 0.1 kg, were from the Laboratory Animal Center of Southwest Medical University [License No: SYXK (CHUAN) 2018-065]. 24 rabbits were randomly divided into the following four groups: sham-operation group, I/R injury followed by CEUS examination at 24-h post-operation group (24-h I/R), I/R injury followed by CEUS examination at 3-d post-operation group (3-d I/R), and I/R injury followed by CEUS examination at 5-d post-operation group (5-d I/R). Prior to surgeries, all rabbits were housed and accommodated for one week with food and water provided *ad libitum*.

### **1.2 Establishment of the animal models**

Surgeries were conducted at room temperature. The hair at the bilateral kidney area was removed, and the skin was exposed. Two-dimensional ultrasound imaging was used to locate the kidneys before surgery. After local anesthesia induced by 3% Pelltobarbitalum Natricum at a dose of 30 mg/kg, the kidney on the right was excised, and the kidney on the left was well separated. For I/R injury groups, left renal artery was clipped with artery clip. Once tissue ischemia was confirmed via the color of the kidney changes from bright red to dark red, as well as by a lack of blood perfusion in the renal parenchyma (as assessed by color Doppler imaging; Figure 1), the artery clip was then maintained for 1 h before being released. Then, the kidney turned from dark red back to bright red, which indicated successful reperfusion. This time was recorded as I/R time. The incision was closed with sutures. For sham-operation groups rabbits were subjected to the same procedures except that kidney on the left was merely exposed—but was untreated—for 1 h before the incision was closed.

### **1.3 Contrast-enhanced ultrasonography (CEUS)**

CEUS imaging was performed via a GE LOGIQ 9 ultrasound machine and a 10-L linear array transducer probe. The probe was fixed at the maximum coronal section of the left kidney. CEUS parameters were set with a low mechanical index (MI) of 0.08, a dynamic range of 50 dB, a depth of 3–4 cm, inclusion of time-gain compensation, and a focus range that was set in the center of a region of interest (ROI). SonoVue (Bracco, Italy) lyophilized powder was used as the contrast agent, which was suspended in 5 ml of normal saline and was mixed well to obtain a microbubble suspension. The dosage of suspension injection is 0.1 ml/kg through the Auricular vein. And then with 1 ml of normal saline to flush the tubes. Dynamic imaging data were continuously recorded for 5 min, saved to disk, and analyzed using TIC analysis software. A circular ROI with a diameter of 3 mm was placed in the parenchyma with the strongest echogenicity. A TIC was generated for each group. The following quantitative parameters were analyzed: the area under the curve (AUC), blood perfusion peak intensity change (A), the curve's peak ascending slope (wash-in slope, WIS), arrival time (AT), and time-to-peak (TTP). To minimize errors, all data were acquired on the same machine using the same protocol, with the same mechanical indices, and the same batch of the contrast agent was used by a single operator.

## 1.4 Renal pathological examinations

Rabbits were euthanized at 24 h, 3 d, and 5 d after I/R injury. The left kidney was quickly excised. One third of the kidney tissue was used for immunohistochemical examination. Histopathological analyses were performed by members in the Department of Pathology at the Affiliated Hospital of Southwest Medical University.

## 1.5 Statistical analysis

Descriptive and inferential statistical analyses were performed using SPSS17.0. Inter- and intra-group differences were compared using one-way analyses of variance (ANOVAs). TIC-derived quantitative indices were analyzed using linear correlation analysis and the correlation coefficient,  $r$ , was calculated.

## 2. Results

Two-dimensional ultrasound imaging was used to detect and assess normal rabbit kidneys, which were bean-shaped and  $2.3 \pm 0.8$  cm in size. The renal capsule was smooth, clear, and hyperechoic. Color Doppler flow imaging (CDFI) of the renal parenchyma revealed the different grades of renal arteries and their corresponding veins. The blood flow in the aorta, segmental arteries, and lobar arteries were visualized with evenly distributed color-coded flow information. However, CDFI was unable to detect any blood flow that was deeper than the renal capsule (Fig. 2).

At 3–5 s after an intravenously delivered bolus injection of contrast agent via the auricular vein, the recorded cine loop was visually inspected. In the sham-operation group, The renal cortex, medulla, renal artery, segmental artery, interlobar artery and arcuate artery were observed in turn (Fig. 3). Within the

following 35–50 s, the enhancement subsided to the background level in the same sequence, with the renal cortex being the last area of complete subsidence. During the peak signal time, the left kidney showed a “fireball-like” enhancement. In the I/R groups, the contrast-agent enhancement and subsidence were both slow, and the “fireball-like” enhancement was not as obvious as that in the sham-operation group. By analyzing the selected renal cortical ROI, the corresponding TIC was obtained. As shown in Figs. 4–8, the TIC of the sham-operation group ascended and descended rapidly, while those of the I/R groups ascended and descended slowly. These results suggested that there was renal hemodynamic dysfunction in the I/R groups.

Table 1  
TIC parameters of the renal cortex in each group ( $\pm s$ ).

Groups	A (dB)	AT (s)	TTP (s)	AUG (dB)	WIS (dB/s)
Sham	15.027 $\pm$ 13.488				
I/R injury					
24 h	16.626 $\pm$ 15.271				
3 d	15.846 $\pm$ 16.233				
5 d	18.655 $\pm$ 15.835				

Table 1: as compared with the sham-operation group, \*P < 0.05, \*\*P < 0.01.

The measured value AUC, TTP, A, AT, and WIS were analyzed among the sham-operation group, 24-h I/R group, 3-d I/R group, and 5-d I/R group (Table 1 and Fig. 9) through One-way ANOVAs. The measured value A, which was not different between any groups ( $P > 0.05$ ), the AT, TTP, AUC, and WIS of the I/R groups were marked difference from those of the sham-operation group ( $P < 0.01$ ). The AT and TTP values reached their peaks at 3 d after I/R injury. Finally, the AUC was not marked difference between the three I/R groups ( $P > 0.05$ ).

In the sham-operation group, the anatomical structures of nephrons were clear. The glomeruli and tubules were well organized. In the 24-h I/R group, the tubular epithelial cells underwent degeneration with characteristic morphological changes, such as increased somatic sizes with cytoplasmic vacuolation (balloon-like changes) and pale staining. Other pathological changes included dilation of the proximal tubules, cellular casts in the distal tubules and collecting ducts, parenchymal edema, and infiltration of inflammatory cells in the renal parenchyma. Compared with the sham operation group, these results demonstrated the renal injury was obvious in the I/R groups (Fig. 10). At 3d after I/R injury,, renal injury was exacerbated and was characterized by coagulative necrosis in proximal tubular epithelial cells, congestive and inflammatory penumbra around the necrotic tissue, dilation of the proximal tubules, cellular casts in the distal tubules, significant parenchymal edema, and extensive inflammatory-cell

infiltration (Fig. 11). At 5 d after I/R injury, the distal tubules were dilated slightly (with a small number of cellular casts), degenerated or necrotic epithelial cells were present, the parenchymal edema was alleviated with focal infiltration of inflammatory cells, and increased neovasculature was found (Fig. 12).

### 3. Discussion

In humans, the kidneys have the most abundant blood supply, receiving roughly 20–25% of cardiac output, and filter approximately 94% of this bloody supply through the cortex. RBF varies under different conditions. Under conditions such as hemorrhagic shock, low cardiac output, or redistribution of systemic blood flow, significant pre-renal arterial contractions lead to rapid and dramatic RBF reduction. CEUS can detect a 15% reduction in human RBF [18]. Cagini et al considered that 2-2.5 min was the best time to observe renal injury after injection of contrast medium [19].

Currently, a nuclear medical scan can examine blood flow to the kidneys. However, its high cost and inability to delineate the dynamic changes of the cortical and medullary blood flow limit its clinical application as a routine test. CDFI has some diagnostic value in the assessment of vascular changes, but it cannot accurately measure blood perfusion in the renal arcuate and smaller arteries. Moreover, CDFI results may vary among different operators. Wei et al reported that CEUS not only detects early hemodynamic changes in a rabbit AKI model but also helps to delineate abnormal changes in renal blood distributions and hemodynamic [20]. Jin et al. examined a number of patients before renal transplantation through contrast-enhanced ultrasound technology, and found that the enhanced parameters reflected certain advantages in monitoring the blood flow perfusion of transplanted kidney, and suggested that this technology may be able to early diagnose acute rejection of renal transplantation. This indicates that CEUS has certain potential in clinical diagnosis and efficacy evaluation of renal diseases, especially those with renal blood circulation changes, but further research is needed [21].

SonoVue is an ideal red-blood-cell tracer [22]. SonoVue has a chemical composition of  $F_6S$ , and a microbubble diameter similar to that of average red-blood-cell diameters; hence, it can flow to all organs and tissues and is then excreted through the respiratory system instead of the urinary system, making it safe for all tissues and organs [23]. After the administration of contrast agent, a TIC can be produced for the ROI within the imaging plane. From the produced TIC, several temporal and amplitude features can be obtained, including AT, TTP, A, AUC, and the WIS [24–25].

These parameters quantitatively evaluate the real-time blood flow characteristics in the capillaries of the renal cortex. The value of AT, which represents the time interval between commencing of contrast-agent administration and when signals start to enhance in the ROI, is determined by the blood flow velocity in renal cortical microvessels. The value of TTP, which is the time interval between the commencing of contrast-agent administration and signals reaching their peaks in the ROI, is determined by the blood flow velocity in renal cortical blood vessels. In the present study, due to the short contrast-agent-filling time and the relatively small sample size, the temporal and amplitude changes of the echogenicity

enhancement in the renal cortex were difficult to differentiate by direct visual inspection alone. Analysis of TICs indicated that the AT and TTP were the slowest at 3 d after I/R injury. This result suggested that it took a long time for the contrast agent to reach the renal capillaries as a consequence of increased resistance in the renal cortical microvasculature. Renal histopathological examinations showed that at 3 d after I/R injury, some of the renal tubular epithelial cells exhibited chromatin condensation, genomic DNA fragmentation, and dissolution of internal nuclear structure, all of which are characteristics of oncotic (coagulative) necrosis. Additionally, there was a congestive and inflammatory penumbra around the necrotic area. Cellular casts were seen in tubular lumens, with interstitial edema and numerous lymphocytic infiltrations. The pathological changes were most significant in the 3-d I/R kidneys. At 3 d after I/R injury, neutrophils and various metabolites not only accumulated within the blood-vessel lumen but also extravasated to cause extensive interstitial edema and to compress small blood vessels. The overall results were increased vascular resistance and reduced blood flow velocity in the microvasculature. WIS represents the average blood velocity and local tissue perfusion rate since the emergence of contrast agent in the ROI. Theoretically, as the TTP prolongs, the TIC curve becomes flat and the WIS is reduced. Changes in WIS are opposite to those of AT and TTP. Our present results further validated that as the AT and TTP were prolonged, the WIS decreased and the TIC became flattened. The WIS was lowest and the ascending of the curve was slowest in the 3-d I/R group, which was followed sequentially by the 24-h I/R group, 5-d I/R group, and the sham group. These results suggested that the value of WIS changed at different time points after I/R injury. The change of WIS showed an opposite trend to that of AT and TTP. The AUC is affected by blood flow velocity and the contrast-agent distribution volume, and is linearly correlated with the blood supply in the renal parenchyma [26]. Theoretically, when the TTP is delayed, the AUC should increase as a result of an increased number of microbubbles entering the ROI. Our present results showed that the I/R groups had significantly greater AUCs than that of the sham-operation group, which were consistent with the aforementioned theory. This phenomenon might be explained by the numerous stagnant microbubbles in the renal capillaries as a result of swelling of the renal medulla, compression of small renal veins, and consequent increase of venous-return resistance. The stasis of renal cortical blood flow is the main reason for the reduced descending slope of the cortical blood-flow curve. The reduction of renal blood perfusion, together with stasis of cortical blood flow, leads to a significantly increased AUC value. In the present study, the AUC values did not significantly differ among the I/R groups, whereas the changes in RBF caused by AKI induced differential degrees of tissue damage among these groups. This discrepancy might be explained by several factors. First, within 5 d of I/R injury, a great number of activated neutrophils adhered to the endothelium of the renal parenchymal venule. Microbubbles could be phagocytosed and subsequently remain intact within these activated neutrophils. It has been demonstrated that phagocytosed microbubbles remain acoustically active and can be detected [20]. Second, renal I/R injury is an irreversible process. The RBF only resumes when necrotic cells are absorbed, or when new blood vessels are formed. Due to the high permeability of neovasculature, reduced cortical blood-flow velocity, and interference from inflammatory cells, the accumulation of microbubbles is not significantly detectable via ultrasound imaging procedures. For these reasons, the AUC is not a suitable parameter for the quantitative evaluation of renal blood volume in renal AKI. In contrast, the A value, which denotes the change in the perfusion peak intensity during the

contrast process, reflects the number of microbubbles in the renal cortex and the change of local blood flow. In the present study, the A value did not differ among the experimental groups, because the A value represented the transient signal intensity instead of an accumulative effect. Therefore, the A value is not a reliable quantitative parameter to monitor changes in blood perfusion following renal I/R injury.

## 4. Conclusions

Hence, the A and AUC offer limited value in the quantitative analysis of renal blood perfusion and in the evaluation of renal functional changes during AKI. However, the specificities and sensitivities of the A and AUC parameters require further investigation. Because previous studies have used different ultrasound machines, contrast agents, durations of recorded CEUS data, sizes/locations of sampling areas, and software packages used for data analysis, there are no established reference values of ultrasonographic parameters for the quantitative evaluation of renal cortical microcirculation and perfusion. To establish well-accepted diagnostic criteria, a larger sample size and standardized operating procedures are needed [20]. In summary, we found that the AT, TTP, and WIS derived from CEUS-acquired TICs represent sensitive indicators that reflect renal blood perfusion, which may be useful for evaluating renal tissue damage at early stages of AKI.

## Abbreviations

A: peak intensity; AKI: acute kidney injury; ANOVAs: one-way analyses of variance; AT: arrival time; AUC: area under the curve; BUN: blood urea nitrogen; CDFI: Color Doppler flow imaging; CEUS: contrast-enhanced ultrasound; H&E: hematoxylin and eosin staining; I/R: ischemia-reperfusion; MI: mechanical index; ROI: a region of interest; ROS: reactive oxygen species; TIC: time-intensity curve; TTP: time-to-peak; WIS: wash-in slope

## Declarations

## Acknowledgements

Not applicable.

## Authors' contributions

YD established the general idea of the study and completed the final draft of this manuscript. ZL determined the detail research scheme and methods, and was responsible for completing the whole research work as well as writing the manuscript. YL, ZT, JL and XX assisted ZL in data acquisition and analysis.

## Funding

This research was supported financially by Doctoral Research Startup Fund of the Affiliated Hospital of Southwest Medical University (16250), Nuclear Medicine and Molecular Imaging Key Laboratory of Sichuan Province (HYX19014), Luzhou Municipal People's Government - Southwest Medical science and technology strategic cooperation projects (2019LZXNYDJ41). Southwest Medical University Youth Fund (12063), Research funding projects of Education Department of Sichuan Province (14ZA0139). Research funding projects of Sichuan Medical Research Law Center (YF16-Q24).

## Availability of data and materials

All the experimental data involved in this study are included in this paper.

## Ethics approval and consent to participate

The animal experiment was approved by the ethics committee of the Affiliated Hospital of Southwest Medical University. All participants agreed to publish the works in Journal of Translational Medicine, and meanwhile share with the experimental data and materials and be responsible for their authenticity.

## Consent for publication

Not applicable.

## Competing Interests

None

## Author details

<sup>1</sup> Department of Ultrasound, the Affiliated Hospital of Southwest Medical University, Luzhou, Sichuan Province, China

<sup>2</sup>Department of medical imaging of Southwest Medical University, Luzhou, Sichuan Province, China

## References

1. Hao Liu,Lei Wang,Xiaodong Weng,Hui Chen,Yang Du,Changhui Diao,et al. Inhibition of Brd4 alleviates renal ischemia/reperfusion injury-induced apoptosis and endoplasmic reticulum stress by blocking Fox O4-mediated oxidative stress. *Redox Biology*. 2019;(24): 101195.  
<https://doi.org/10.1016/j.redox.2019.101195>.

2. Ali T, Khan I, Simpson W, Prescott G, Townend J, Smith W, et al. Incidence and outcomes in acute kidney injury: a comprehensive population-based study. *J Am Soc Nephrol.* 2007;(18):1292–1298. <https://doi.org/10.1681/ASN.2006070756>.
3. Bellomo R, Kellum JA, Ronco C. Acute kidney injury. *Lancet.* 2012;(380): 756–766. [https://doi.org/10.1016/S0140-6736\(11\)61454-2](https://doi.org/10.1016/S0140-6736(11)61454-2).
4. Rewa O, Bagshaw SM. Acute kidney injury—epidemiology, outcomes and economics. *Nat Rev Nephrol.* 2014; (10):193–207. <https://doi.org/10.1038/nrneph.2013.282>.
5. Nath KA, Norby SM. Reactive oxygen species and acute renal failure. *Am J Med.* 2000; (109):665–678. [https://doi.org/10.1016/S0002-9343\(00\)00612-4](https://doi.org/10.1016/S0002-9343(00)00612-4).
6. Yang L, Besschetnova TY, Brooks CR, Shah JV, Bonventre JV. Epithelial cell cycle arrest in G2/M mediates kidney fibrosis after injury. *Nat Med.* 2010; (16):535–543. <https://doi.org/10.1038/nm.2144>.
7. Ferenbach DA, Bonventre JV. Mechanisms of maladaptive repair after AKI leading to accelerated kidney ageing and CKD. *Nat Rev Nephrol.* 2015;(11):264–276. <https://doi.org/10.1038/nrneph.2015.3>.
8. Basile DP, Bonventre JV, Mehta R, Nangakum M, Unwin R, Rosner MH, et al. Progression after AKI: understanding maladaptive repair processes to predict and identify therapeutic treatments. *J Am Soc Nephrol.* 2016; (27): 687–697. <https://doi.org/10.1681/ASN.2015030309>.
9. Kasap B, Soylu A, Türkmen M, Kavukcu S. Relationship of increased renal cortical echogenicity with clinical and laboratory findings in pediatric renal disease. *J Clin Ultrasound* 2006, (34):339-342. <https://doi.org/10.1002/jcu.20243>.
10. Ko GJ, Grigoryev DN, Linfert D, Jang HR, Watkins T, Cheadle C, Racusen L, Rabb H. Transcriptional analysis of kidneys during repair from AKI reveals possible roles for NGAL and KIM-1 as biomarkers of AKI-to-CKD transition. *Am J Physiol Renal Physiol.* 2010;( 298): F1472-1483. <https://doi.org/10.1152/ajprenal.00619.2009>.
11. Haase M, Devarajan P, Haase-Fielitz A, Bellomo R, Cruz DN, Wagener G, et al. The outcome of neutrophil gelatinase-associated lipocalin-positive subclinical acute kidney injury: a multicenter pooled analysis of prospective studies. *J Am Coll Cardiol.* 2011; 57(17):1752-1761. <https://doi.org/10.1016/j.jacc.2010.11.051>.
12. Ronco C, Chawla LS. Glomerular and tubular kidney stress test: new tools for a deeper evaluation of kidney function. *Nephron.* 2016; 134(3): 191-194. <https://doi.org/10.1159/000449235>.
13. Wei Cao, Shuang Cui, Li Yang, Chunyi Wu, Jian Liu, Fang Yang, et al. Contrast-Enhanced Ultrasound for Assessing Renal Perfusion Impairment and Predicting Acute Kidney Injury to Chronic Kidney Disease Progression. *Antioxid Redox Signal.* 2017(00): 1-15. <https://doi.org/10.1089/ars.2017.7006>.
14. Honore PM, Jacobs R, Waele E, D'Iltoer M, Spapen HD, et al. Renal blood flow and acute kidney injury in septic shock: an arduous conflict that smolders intrarenally?. *Kidney Int.* 2016; 90(1):22-24. <https://doi.org/10.1016/j.kint.2016.03.025>.

15. Schneider A, Johnson L, Goodwin M, Schelleman A, Bellomo R. Bench-to-bedside review: contrast enhanced ultrasonography—a promising technique to assess renal perfusion in the ICU. *Crit Care*. 2011;15(3):157. <https://doi.org/10.1186/cc10058>.
16. Kiryluk K, Bombardieri AS, Cheng YL, Xu K, Camara PG, Rabadan R, et al. Precision Medicine for Acute Kidney Injury (AKI): Redefining AKI by Agnostic Kidney Tissue Interrogation and Genetics. *Semin Nephrol*. 2018; 38(1):40-51. <https://doi.org/10.1016/j.semnephrol.2017.09.006>.
17. Iliescu R, Fernandez SR, Kelsen S, Maric C, Chade AR. Role of renal microcirculation in experimental renovascular disease. *Nephrol Dial Transplant*. 2010;25(4):1079-87. <https://doi.org/10.1093/ndt/gfp605>.
18. Schneider AG, Lucie H, Grégoire W, Nicolas G, Marc M, Jean-Yves M, et al. Renal perfusion evaluation with contrast enhanced ultrasonography. *Nephrol Dial Transplant*. 2012;27(2): 674-681. <https://doi.org/10.1093/ndt/gfr345>.
19. Cagini L, Gravante S, Malaspina CM, Cesarano E, Giganti M, Rebonato A, et al. Contrast enhanced ultrasound (CEUS) in blunt abdominal trauma. *Critical Ultrasound Journal*. 2013; 5(1):S9. <https://doi.org/10.1186/2036-7902-5-S1-S9>.
20. K Wei, E Le, J P Bin, M Coggins, J Thorpe, S Kaul, et al. Quantification of renal blood flow with contrast-enhanced. *J Am Coll Cardiol*. 2001;37(4):1135-1140. [https://doi.org/10.1016/S0735-1097\(00\)01210-9](https://doi.org/10.1016/S0735-1097(00)01210-9).
21. Jin Y, Yang C, Wu S, Zhou S, Ji Z, Zhu T, et al. A novel simple noninvasive index predict renal transplant acute rejection by contrast-enhanced ultrasonography. *Transplantation*. 2015;99(3):636-641. <https://doi.org/10.1097/TP.0000000000000382>.
22. Quai E. Microbubble Ultrasound contrast agents: an update. *Eur Radiol*. 2007;17(8):199-5-2008. <https://doi.org/10.1007/s00330-007-0623-0>.
23. Li Xing, Rui Cui, Lei Peng, Jing Ma, Xiao Chen, Ru-Juan Xie, et al. Mesenchymal stem cells, not conditioned medium contribute to kidney repair after ischemia-reperfusion injury. *Stem Cell Res Ther*. 2014, 59(4):1-12. <https://doi.org/10.1186/scrt489>.
24. Schwarz KQ, Bezante GP, Chen X, Mottley JG, Schlieff R. Volumetric arterial flow quantification using methods: Radio frequency, video and Doppler. *Ultrasound Med Biol*. 1993; 19(6): 447-460. [https://doi.org/10.1016/0301-5629\(93\)90121-4](https://doi.org/10.1016/0301-5629(93)90121-4).
25. Wiesmann M, Bergmann-Köster CU, Kreft B, Stöckelhuber M, Gehl HB, Stöckelhuber BM. Renal perfusion imaging using contrast-enhanced phase-inversion ultrasound. *Clin Nephrol*. 2004; 62(6): 423-431. <https://doi.org/10.5414/cnp62423>.
26. Sonja Brennan, Yogavijayan Kandasamy. Ultrasound Imaging of the Renal Parenchyma of Premature Neonates for the Assessment of Renal Growth and Glomerulomegaly. *Ultrasound Med Biol*. 2017;43(11):2546-2549. <https://doi.org/10.1016/j.ultrasmedbio.2017.06.033>.

## Figures



**Figure 1**

The left kidneys were isolated by a non-invasive blood-vessel clip, during which the kidney changed rapidly from bright red to dark red.

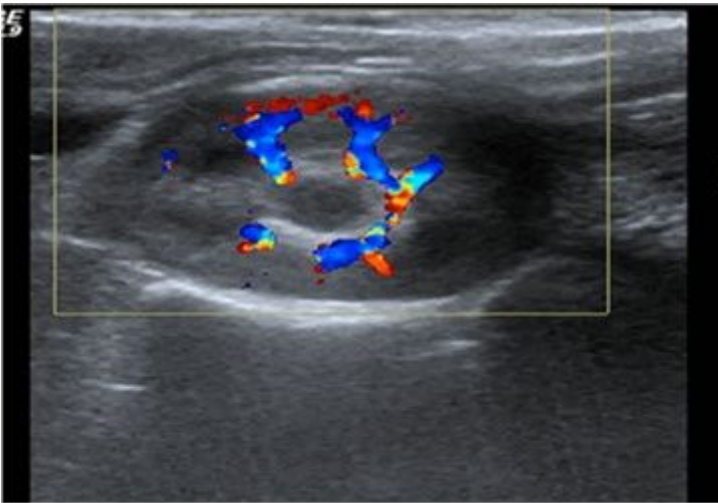


**Figure 2**

CDFI was used to detect renal arterial blood flow in normal rabbits, but this detection barely reached beyond the renal capsule.

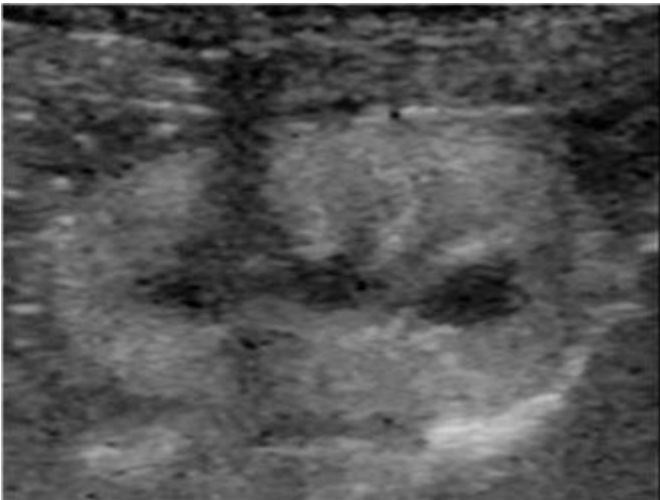


**Figure 3**

Ultrasound contrast-agent began to appear in renal cortex at 5 seconds after administration.

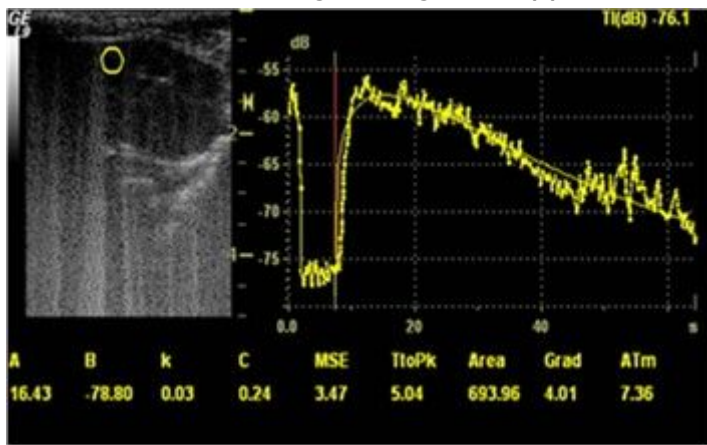


Figure 4

Ultrasound contrast-agent began to appear in renal medulla at 7 seconds after administration.

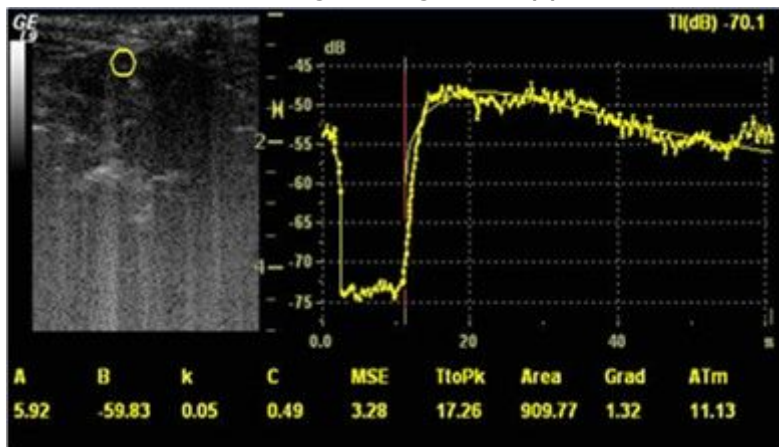
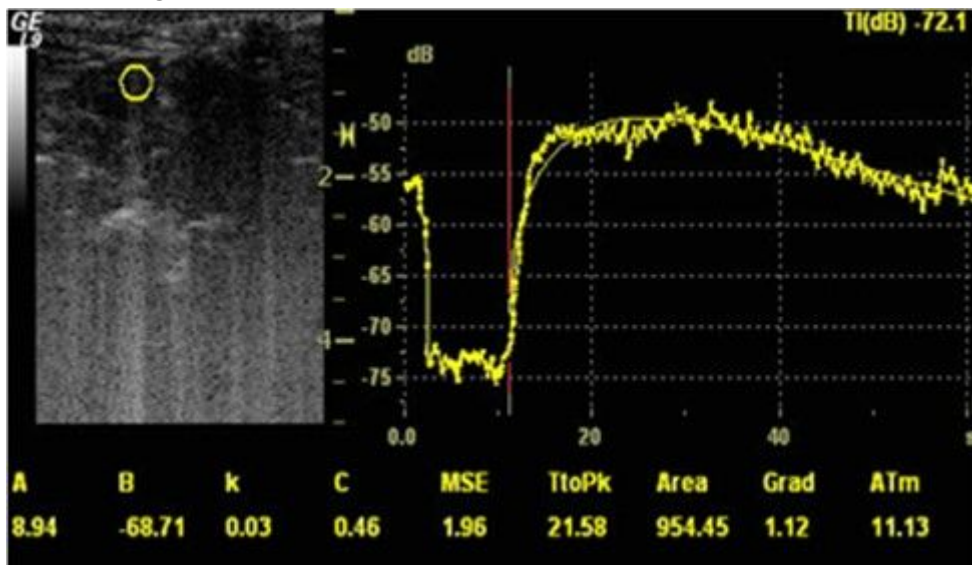


Figure 5

The TIC of the renal cortex in the sham-operation group is shown, indicating a rapid ascending and descending curve.



**Figure 6**

The TIC of the renal cortex in the 24-h I/R group is shown, indicating a slower ascending and descending curve.

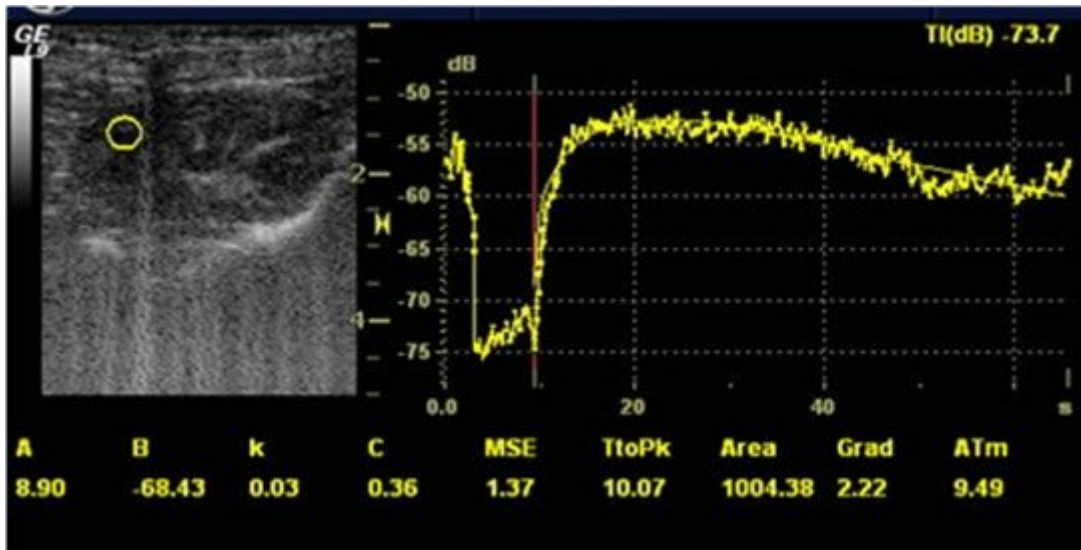


**Figure 7**

The TIC of the renal cortex in the 3-d I/R group is shown.

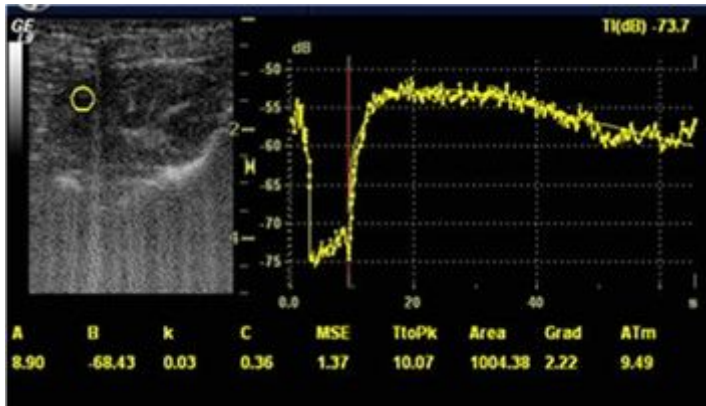


**Figure 8**

The TIC of the renal cortex in the 5-d I/R group is shown.

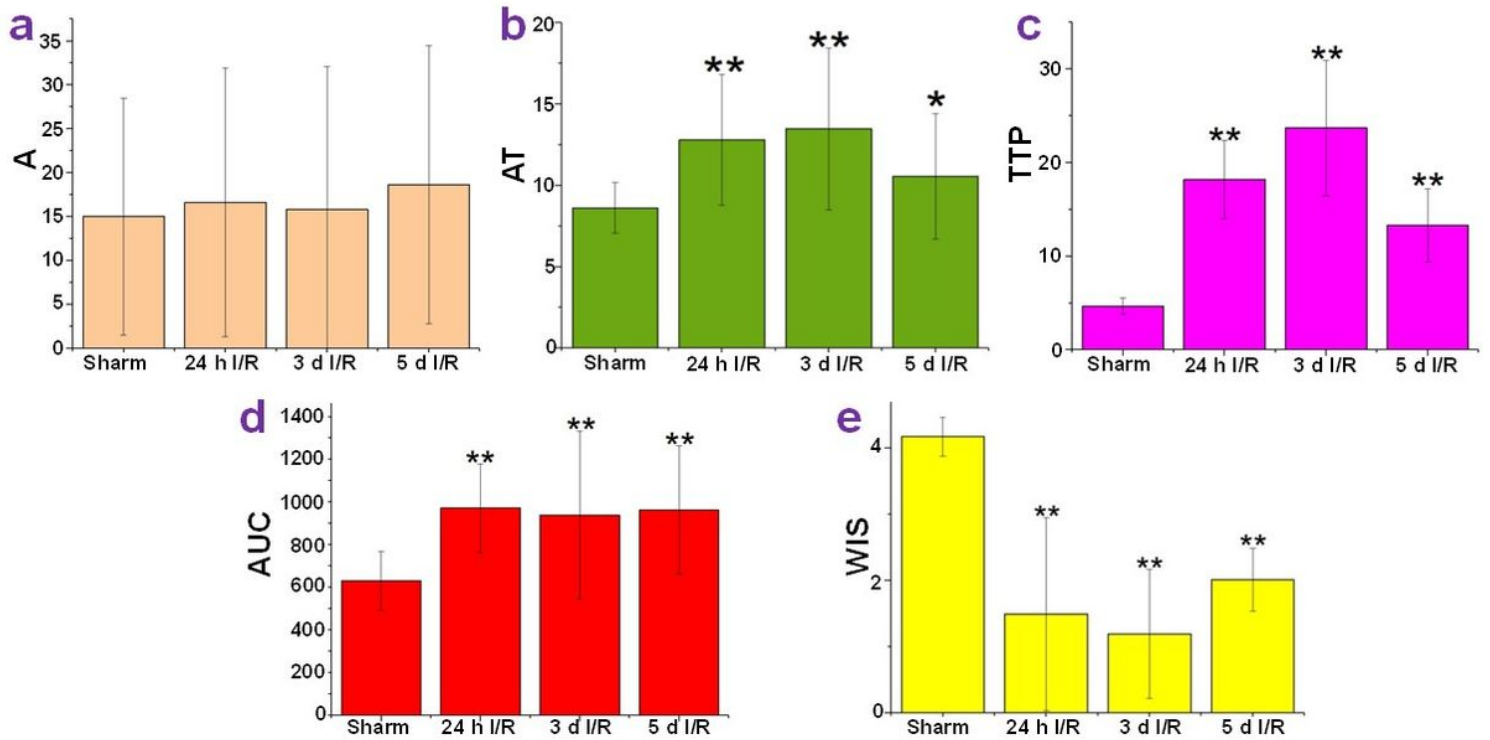


**Figure 9**

Analysis of quantitative CEUS parameters derived from TICs. (a) The A values were not different among the groups ( $P > 0.05$ ); (b and c) The AT and TTP values of the I/R groups were significantly greater than those of the sham-operation group. The AT and TTP values peaked at 3 d after I/R injury and partially decreased at 5 d after I/R injury. (d) The AUC values of the I/R groups were significantly greater than that of the sham-operation group. However, the AUCs did not differ among the I/R groups. (e) The WIS of the sham-operation group was significantly greater than that of the I/R groups, with the 3-d I/R group having the lowest WIS (\* $P < 0.05$ , \*\* $P < 0.01$ ).

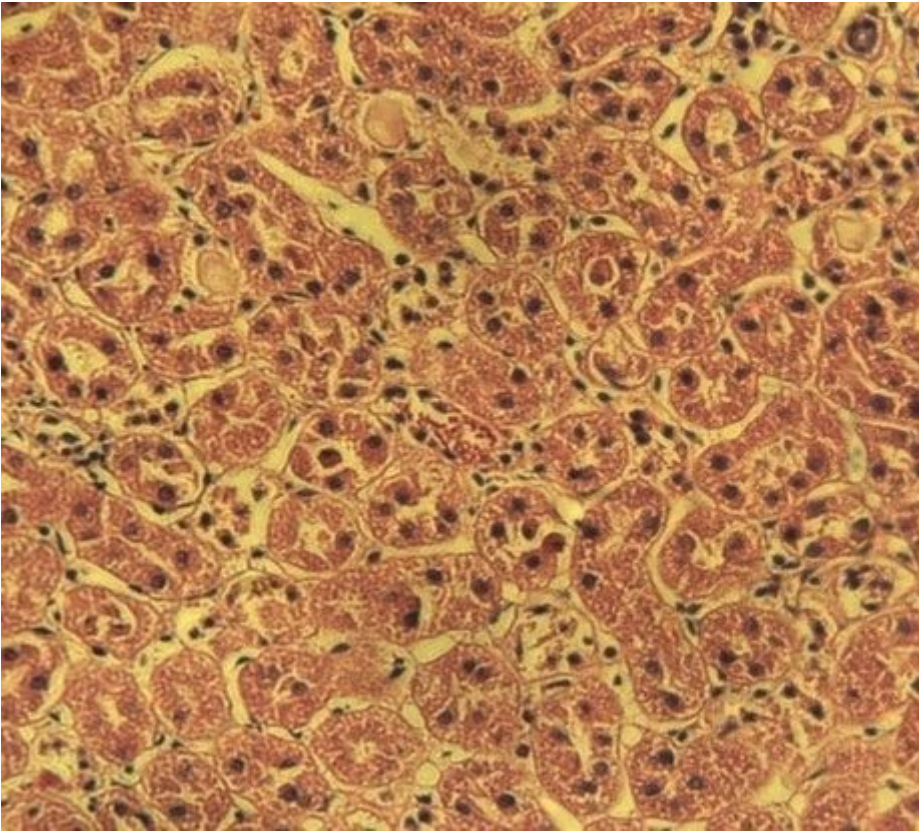


**Figure 10**

The renal histopathology of the 24-h I/R group is shown (200× magnification).

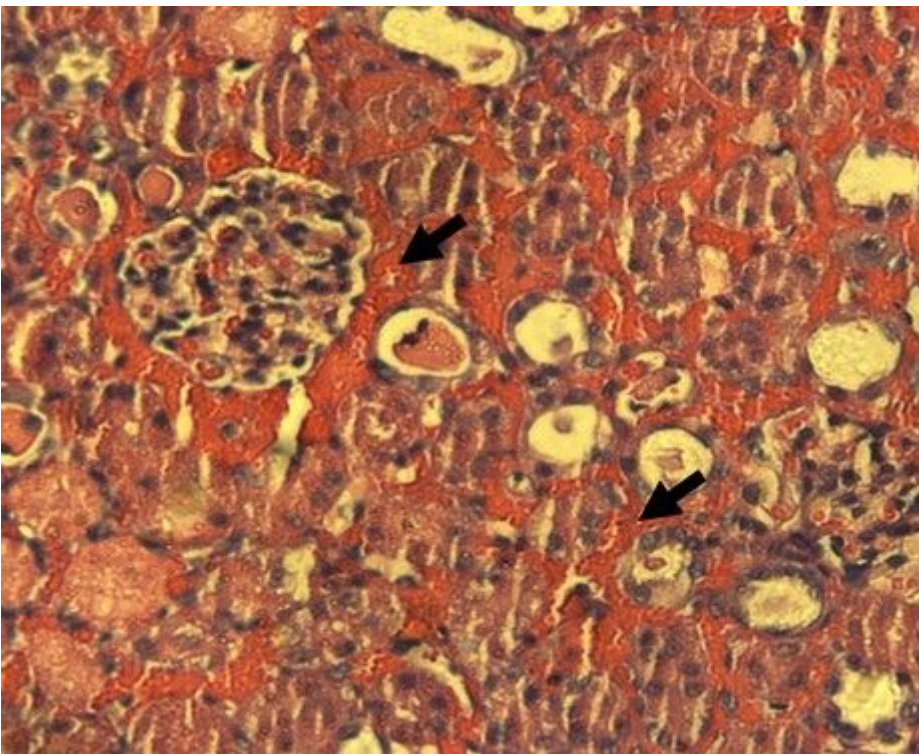


**Figure 11**

The renal histopathology of the 3-d I/R group is shown (200× magnification).

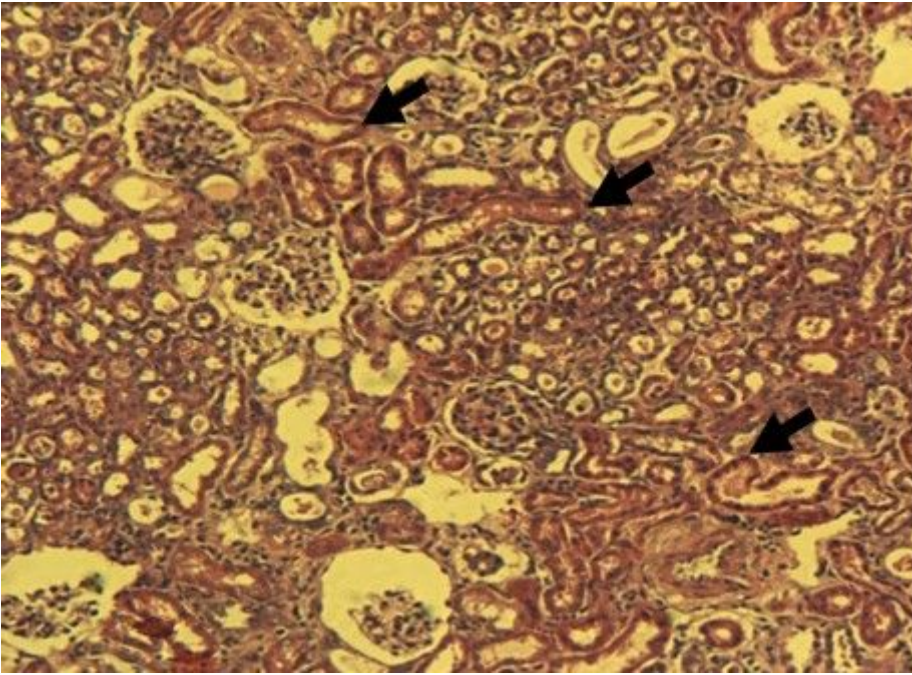


**Figure 12**

The renal histopathology of the 5-d I/R group is shown (200× magnification).